



# Comparison of lithium iron phosphate blended with different carbon sources for lithium battery electrodes

Yiming Zhang<sup>1</sup>

Received: 3 April 2023 / Revised: 30 July 2023 / Accepted: 8 August 2023 / Published online: 23 August 2023  
© The Author(s), under exclusive licence to Korean Carbon Society 2023

## Abstract

In response to the growing demand for high-performance lithium-ion batteries, this study investigates the crucial role of different carbon sources in enhancing the electrochemical performance of lithium iron phosphate (LiFePO<sub>4</sub>) cathode materials. Lithium iron phosphate (LiFePO<sub>4</sub>) suffers from drawbacks, such as low electronic conductivity and low lithium-ion diffusion coefficient, which hinder its industrial development. Carbon is a common surface coating material for LiFePO<sub>4</sub>, and the source, coating method, coating amount, and incorporation method of carbon have a significant impact on the performance of LiFePO<sub>4</sub> materials. In this work, iron phosphate was used as the iron and phosphorus source, and lithium carbonate was used as the lithium source. Glucose, phenolic resin, ascorbic acid, and starch were employed as carbon sources. Ethanol was utilized as a dispersing agent, and ball milling was employed to obtain the LiFePO<sub>4</sub> precursor. Carbon-coated LiFePO<sub>4</sub> cathode materials were synthesized using the carbothermal reduction method, and the effects of different carbon sources on the structure and electrochemical performance of LiFePO<sub>4</sub> materials were systematically investigated. The results showed that, compared to other carbon sources, LiFePO<sub>4</sub> prepared with glucose as the carbon source not only had a higher discharge specific capacity but also better rate cycle performance. Within a voltage range of 2.5–4.2 V, the initial discharge specific capacities at 0.1, 0.5, and 1 C rates were 154.6, 145.6, and 137.6 mAh/g, respectively. After 20 cycles at a 1 C rate, the capacity retention rate was 98.7%, demonstrating excellent electrochemical performance.

**Keywords** Lithium iron phosphate · Positive electrode material · Carbon source · Coating · Performance

## 1 Introduction

Owing to their elevated operating voltage, exceptional specific energy, extended service life, absence of memory effects, and minimal environmental impact, lithium-ion batteries are extensively employed in handheld electronic gadgets, such as smartphones, digital cameras, and notebook computers [1, 2]. These batteries have also been widely utilized as alternatives to fossil fuels in novel energy automobiles and energy storage systems. In lithium-ion batteries, the cathode material not only comprises the largest portion of the battery's expense, but its efficiency also significantly influences the overall electrochemical performance and safety of the battery [3–5]. At present, widely researched cathode materials encompass lithium cobalt oxide, lithium

nickel cobalt manganese oxide, lithium nickel cobalt aluminum oxide ternary compounds, lithium manganese oxide, and lithium iron phosphate [6–8]. Among these, olivine-structured lithium iron phosphate (LiFePO<sub>4</sub>) cathode materials have emerged as a focal point of research and development in numerous nations due to their plentiful supply, extended cycling durability, and superior safety [9]. They are commonly employed in innovative energy automobiles, energy storage systems, uninterruptible power sources, and electric appliances, offering a vast market potential. However, the low electrical conductivity of pure LiFePO<sub>4</sub> cathode materials limits their rate and cycling performance [10]. To address this issue, many researchers have conducted modification studies, such as ion doping, surface coating, and particle nanosizing [11]. In particular, surface carbon coating not only enhances the conductivity of LiFePO<sub>4</sub> cathode materials but also suppresses particle growth, attenuates electrode polarization effects, and ultimately improves their rate performance and extends their cycle life [12, 13].

✉ Yiming Zhang  
yiming19970308@163.com

<sup>1</sup> Sunwoda Electric Vehicle Battery Co, Shenzhen 518106, Guangdong, China

It is well known that the intrinsic electrical conductivity of  $\text{LiFePO}_4$  is only  $10^{-9}$  to  $10^{-10}$   $\text{cm}^2/\text{S}$ , compared to the  $10^{-6}$   $\text{cm}^2/\text{S}$  of carbon anode materials, making this low conductivity a bottleneck for its development. Adding an appropriate conductive agent or performing effective carbon coating during the preparation of  $\text{LiFePO}_4$  is a crucial means of improving its electrical conductivity [14–16]. Carbon coating modification generally involves coating the exterior of  $\text{LiFePO}_4$  crystals with a layer of highly conductive carbon material, which provides an electron tunnel for the electron transfer of lithium iron phosphate and weakens the polarization effect, thereby improving the corresponding electrochemical performance [17–20]. The carbon coating process involves the carbonization reaction of carbon source materials during high-temperature sintering, causing structural changes and a certain degree of graphitization, forming a carbon layer tightly wrapped around the exterior of  $\text{LiFePO}_4$  crystals, predominantly resulting in a core–shell structure [21–23]. Carbon coating was initially proposed by Armand et al. [24], and after the carbon coating, the electrochemical reaction kinetics of  $\text{LiFePO}_4$  were improved, making the actual specific capacity of the pure material at room-temperature approach its theoretical specific capacity (170 mAh/g). When designing carbon-based  $\text{LiFePO}_4$  cathode materials, the key issue is controlling the amount of carbon added, as adding high surface area carbon nanomaterials can reduce the tap density and subsequently decrease their energy density. Research suggests that the ideal carbon content in composite materials is 1% to 3% of the total mass; the next consideration is the structure of the nanocomposite material, which should balance a reduction in porosity while providing sufficient space for lithium-ion diffusion within the electrode. Zhao et al. [25] found that when  $\text{LiFePO}_4/\text{C}$  exhibited a pomegranate-like microspherical structure, the battery demonstrated excellent processability and low-temperature performance. From the perspective of surface modification, the impact of carbon coating on the material is mainly manifested in the formation of an electron-conductive layer on its surface after coating, which enhances the conductivity between particles and within particles, provides electron tunnels for  $\text{LiFePO}_4$ , reduces battery polarization, compensates for charge balance during lithium-ion deintercalation, and improves the conductivity of the active material. Carbon materials can reduce  $\text{Fe}^{3+}$  to  $\text{Fe}^{2+}$  at high temperatures, hindering the formation of trivalent iron and improving product purity. This process also suppresses grain growth, making the particle size more uniform, with minimal agglomeration, effectively controlling particle size and enabling nanosizing.

Selecting an appropriate carbon source during the carbon coating modification process has a significant impact on the improvement of  $\text{LiFePO}_4$  electrochemical performance. The properties of different carbon sources affect the shape,

structure, and coating conditions of the carbon layer during the carbonization process, making the selection of carbon source types and understanding the carbonization characteristics of different carbon sources particularly important. In the process of carbon coating, prevalent carbon sources can be categorized into inorganic carbon sources, organic carbon sources, and organic polymer carbon sources. Inorganic carbon sources encompass various forms of carbon materials such as carbon black, carbon nanotubes, and graphene; organic carbon sources involve organic compounds like sucrose, glucose, starch, and citric acid; organic polymer carbon sources consist of polymer carbon sources created through in situ polymerization of organic monomers, including polyaniline, polyacrylic acid, and polyvinyl alcohol. In this research, iron phosphate served as the iron and phosphorus source, lithium carbonate functioned as the lithium source, and a carbon source was incorporated, using alcohol as a dispersing agent to produce the lithium iron phosphate precursor via ball milling. Carbon-coated lithium iron phosphate cathode materials were fabricated employing a carbothermal reduction technique, and the influence of carbon sources on the structure and electrochemical properties of lithium iron phosphate materials was comprehensively examined.

## 2 Experimental

Lithium carbonate (purity > 99%), iron phosphate (purity > 98%), and the selected carbon sources (glucose, phenolic resin, ascorbic acid, and starch) were used in this study. The lithium carbonate and iron phosphate were sourced from Lingchuan Xianke Chemical Co. Ltd. Lithium carbonate, iron phosphate, and carbon source were weighed according to stoichiometric proportions and placed in a ball mill jar. Anhydrous ethanol was added, with a ball-to-powder mass ratio of 4:1 and a solid content of 45%. The mixture was ball milled at 500 rpm for 10 h, and then dried at 80 °C to obtain the precursor. The ground precursor was placed in a tube furnace and heated under a nitrogen atmosphere to 600 °C for 6 h and then to 800 °C for 5 h to synthesize carbon-coated lithium iron phosphate cathode materials (LFP/C), controlling the carbon content in the final lithium iron phosphate product to  $(2.5 \pm 0.1)\%$ . The carbon sources used here were glucose, phenolic resin, ascorbic acid, and starch, denoted as LFP/G, LFP/P, LFP/A, and LFP/S, respectively.

X-ray diffraction analysis was performed on the samples using an X'Pert PRO X-ray diffractometer with a  $\text{CuK}\alpha$  radiation source, graphite monochromator, tube voltage of 40 kV, tube current of 0.2 A, scanning rate of 8 (°)/min, and scanning range of 10°–70°. The sample morphology was characterized using a Sirion200 field emission scanning

electron microscope. High-precision Neware battery test system (5 V/5 mA) was used for charge–discharge testing of the battery at different rates, with a voltage range of 2.5–4.2 V. Cyclic voltammetry and electrochemical impedance spectroscopy were performed using an Ivium Stat electrochemical workstation, with a cyclic voltammetry scanning voltage range of 2.5–4.2 V and scanning rate of 0.1 mV/s, and an impedance frequency range of  $10^5$  to  $10^{-2}$  Hz. Carbon content was measured using an HH2200A high-frequency infrared carbon–sulfur analyzer. All tests were conducted at room temperature.

LFP/C as the cathode active material, acetylene black (battery grade) as the conductive agent, and polyvinylidene fluoride (battery grade) as the binder were mixed in a mass ratio of 8:1:1. The mixture was combined with N-methylpyrrolidone (battery grade) to form a slurry, uniformly coated at approximately  $7 \text{ mg/cm}^2$  onto a 20  $\mu\text{m}$ -thick aluminum foil (battery grade), cut into 12 mm-diameter discs, and vacuum dried at 80 °C for 12 h. A CR2016 button cell was assembled using metallic lithium (battery grade) as the anode, Celgard 2400 as the separator, and 1 M  $\text{LiPF}_6$  in ethylene carbonate + dimethyl carbonate (volume ratio 1:1, battery grade) as the electrolyte, all in a glove box filled with argon gas.

### 3 Results and discussion

Figure 1 exhibits the XRD patterns of  $\text{LiFePO}_4/\text{C}$  synthesized using different carbon sources. From the figure, it can be observed that the main diffraction peaks of  $\text{LiFePO}_4/\text{C}$  synthesized with different carbon sources are consistent with the standard lithium iron phosphate card (JCPDS #40-1499) [26]. No impurity peaks are present, and the peak shapes are sharp, indicating good crystallinity. This suggests that pure-phase lithium iron phosphate can be prepared using different

carbon sources [27]. The absence of diffraction peaks for carbon in all four samples implies that carbon exists in an amorphous form [28].

Figure 2 exhibits the first charge–discharge curves of lithium iron phosphate prepared using different carbon sources at a 0.1 C rate ( $1 \text{ C} = 170 \text{ mA/g}$ ) within the voltage range of 2.5–4.2 V. All four samples exhibit good charge–discharge plateaus with very gentle voltage variations. The lithium iron phosphate prepared with glucose as the carbon source has a charge plateau at 3.462 V and a discharge plateau at 3.398 V, with a voltage difference ( $\Delta E$ ) of 0.036 V, indicating no significant electrochemical polarization. In contrast, the sample prepared with starch as the carbon source exhibits more significant polarization, possibly due to the longer molecular chains of starch. The carbon generated during thermal decomposition may not uniformly coat the lithium iron phosphate material, which could increase the material's electronic conductivity on one hand but might also decrease the ionic conductivity and lead to increased polarization on the other hand. At a 0.1 C rate, the charge capacities of LFP/G, LFP/P, LFP/A, and LFP/S are 164.5, 147.3, 162.6, and 157.1 mAh/g, respectively, while their discharge capacities are 154.6, 136.4, 155.8, and 148.0 mAh/g, respectively.

Figure 3 shows the cycling performance of lithium iron phosphate prepared using different carbon sources at discharge rates of 0.1, 0.2, 0.5, 1, and 3 C. Within the voltage range of 2.5–4.2 V during cycling, the LFP/G sample prepared with glucose as the carbon source has discharge capacities of 154.6, 152.0, 145.6, 137.6, and 121.9 mAh/g at 0.1, 0.2, 0.5, 1, and 3 C rates, respectively. After 20 cycles at 1 C rate, the capacity retention is 98.7%, demonstrating excellent electrochemical performance. The LFP/P sample prepared with ascorbic acid as the carbon source shows an initial increase in capacity during the first few cycles, reaching 156.7 mAh/g after five cycles, and a 1 C rate discharge

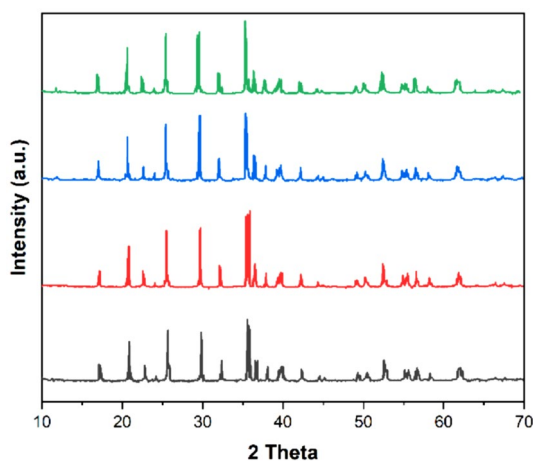


Fig. 1 XRD patterns of LFP/G, LFP/P, LFP/A, and LFP/S

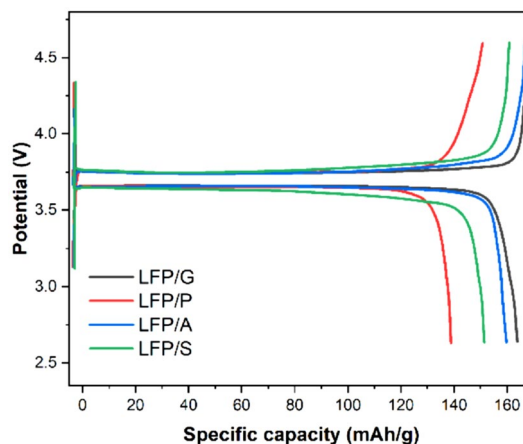
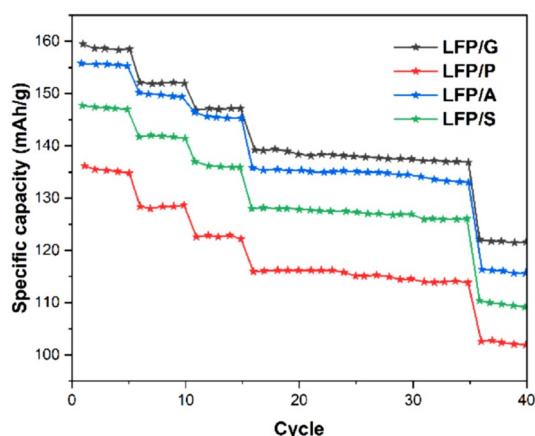


Fig. 2 Initial charge and discharge curve of LFP/G, LFP/P, LFP/A, and LFP/S



**Fig. 3** Cyclic performance of LFP/G, LFP/P, LFP/A, and LFP/S at different rates

capacity of 135.8 mAh/g, with a capacity retention of 98.0% after 20 cycles. The cycling performance of lithium iron phosphate materials prepared with glucose and ascorbic acid as carbon sources at different rates is superior to those prepared with starch and phenol–formaldehyde resin as carbon sources.

Figure 4 shows the SEM images at 50,000 $\times$  magnification of lithium iron phosphate prepared using different carbon sources. From the images, it can be observed that all four samples exhibit some degree of aggregation. The lithium iron phosphate material prepared using glucose has a primary particle size of approximately 300 nm, with a well-defined morphology and a quasi-spherical shape [29]. This may be attributed to the even distribution of conductive carbon, both internally and externally, within the lithium iron phosphate during the pyrolysis of glucose under a nitrogen atmosphere, which effectively inhibits the growth of lithium

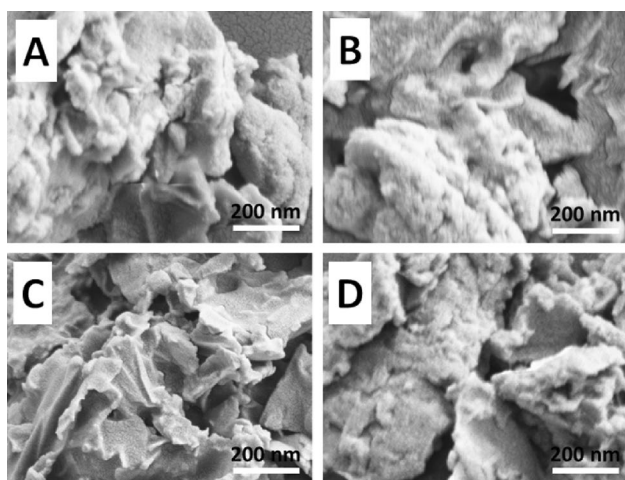
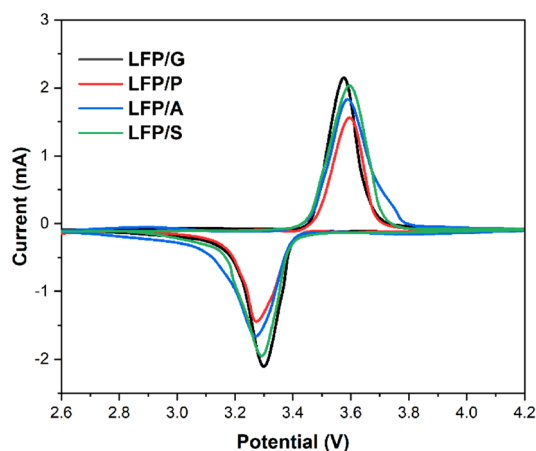


**Fig. 4** SEM images of A LFP/G, B LFP/P, C LFP/A, and D LFP/S

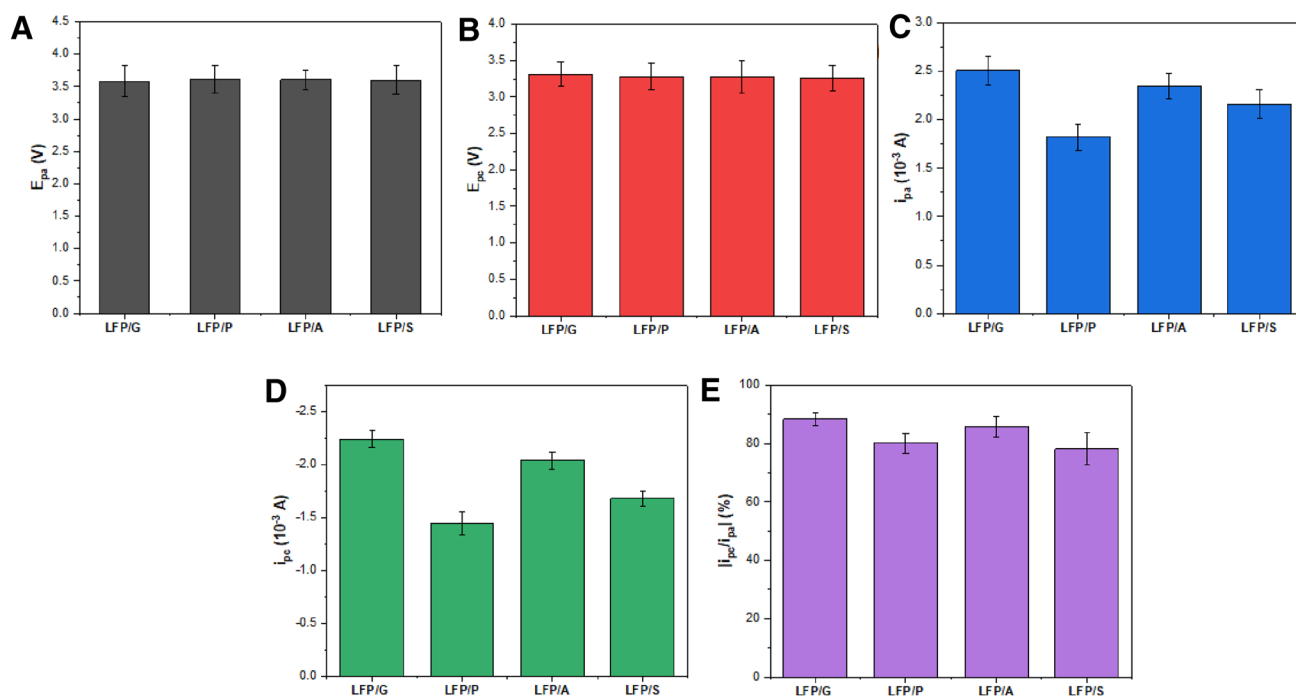
iron phosphate, resulting in a more uniform particle-size distribution [30]. In comparison, LFP/A also has a smaller particle size, but the distribution is not very uniform; the agglomeration phenomenon in LFP/P and LFP/S is more severe.

Figure 5 shows the cyclic voltammograms of lithium iron phosphate prepared using different carbon sources, with a voltage range of 2.5 to 4.2 V and a scan rate of 0.1 mV/s. The voltammograms clearly depict a pair of relatively symmetric redox peaks for each sample, corresponding to the deintercalation of  $\text{Li}^+$  ions and the conversion process between  $\text{Fe}^{2+}$  and  $\text{Fe}^{3+}$ , which are indicative of typical two-phase reaction characteristics [31]. In cyclic voltammetry, the peak potential difference  $|E_p| = E_{pc} - E_{pa}$  and the peak current ratio  $|i_{pc}/i_{pa}|$  serve as important criteria for assessing the reversibility of the charge–discharge process in the material. Figure 6 presents the peak potential differences and peak current ratios for each sample, revealing that LFP/G has the smallest  $E_p$  value of 0.28 V and the highest  $i_{pc}/i_{pa}$  value of 88.5% [32]. This indicates that lithium iron phosphate prepared using glucose as a carbon source exhibits the least polarization and excellent reversibility.

Figure 7 displays the EIS plots of lithium iron phosphate prepared using four different carbon sources. The impedance spectra can be observed to consist of the impedance ( $R_s$ ) associated with  $\text{Li}^+$  migration on the cathode surface film, the semicircle representing the charge transfer resistance ( $R_{ct}$ ) controlled by electrochemical steps [33], and the straight line indicating the Warburg impedance ( $Z_w$ ) arising from  $\text{Li}^+$  diffusion in the solid phase. The  $R_s$  values for lithium iron phosphate prepared using the four carbon sources do not differ significantly, suggesting good stability of the cathode surface film. Notably, the lithium iron phosphate prepared using glucose as the carbon source exhibits the smallest  $R_{ct}$  value of 62.66  $\Omega$ , indicating minimal impedance for  $\text{Li}^+$  deintercalation and intercalation.



**Fig. 5** CV curves of LFP/G, LFP/P, LFP/A, and LFP/S



**Fig. 6** A  $E_{pa}$ , B  $E_{pc}$ , C  $i_{pa}$ , D  $i_{pc}$ , and E  $i_{pc}/i_{pa}$  of CV curves

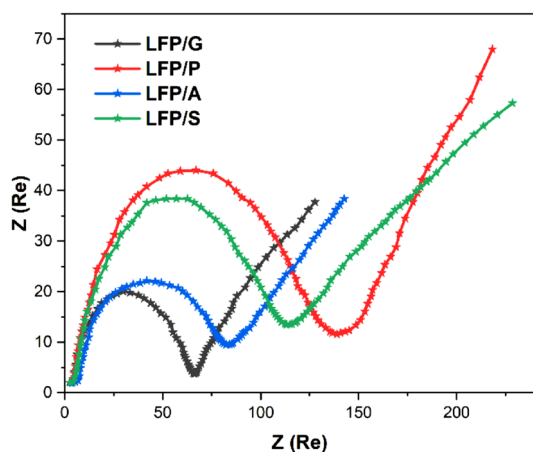


**Fig. 7** EIS plots of LFP/G, LFP/P, LFP/A, and LFP/S

Simultaneously, it has the largest  $i_0$  value, implying the lowest resistance to electrode reactions and a more facile reaction process [34].

In comparison with previous works in this field, the study investigated the effects of different carbon sources on the performance of carbon-coated  $\text{LiFePO}_4$  cathode materials. The results demonstrated that  $\text{LiFePO}_4$  prepared with glucose as the carbon source exhibited superior electrochemical performance, with a higher discharge specific capacity and better rate cycle performance compared to  $\text{LiFePO}_4$

materials prepared using other carbon sources, such as phenolic resin, ascorbic acid, and starch [35–37].

## 4 Conclusion

In summary, carbon-coated lithium iron phosphate composite materials were synthesized using iron phosphate as the iron and phosphorus source, lithium carbonate as the lithium source, and glucose, phenolic resin, ascorbic acid, and starch as carbon sources, respectively. The results demonstrate that all obtained products are olivine-type lithium iron phosphate, with glucose as the carbon source yielding materials with smaller and more uniformly distributed particle sizes. Compared to other carbon sources, lithium iron phosphate prepared with glucose as the carbon source not only exhibits a higher discharge specific capacity but also better rate cycling performance. In the voltage range of 2.5–4.2 V, the initial discharge specific capacities at 0.1, 0.5, and 1C rates are 154.6, 145.6, and 137.6 mAh/g, respectively. Notably, after 20 cycles at a 1C rate, the capacity retention is 98.7%, indicating excellent electrochemical performance.

**Author contributions** YZ conducted all works for this paper. YZ has read and agreed to the published version of the manuscript.

**Funding** None.



**Data availability** The data that support the findings of this study are available from the corresponding author upon reasonable request.

## Declarations

**Conflict of interest** The corresponding author states that there is no conflict of interest

## References

- Qu J, Liu F, Ma Y, Fan J (2019) A neural-network-based method for RUL prediction and SOH monitoring of lithium-ion battery. *IEEE Access* 7:87178–87191
- Manthiram A (2020) A reflection on lithium-ion battery cathode chemistry. *Nat Commun* 11:1550
- Xie J, Lu Y-C (2020) A retrospective on lithium-ion batteries. *Nat Commun* 11:2499
- Weiss M, Ruess R, Kasnatscheew J, Levartovsky Y, Levy NR, Minnmann P, Stolz L, Waldmann T, Wohlfahrt-Mehrens M, Aurbach D (2021) Fast charging of lithium-ion batteries: a review of materials aspects. *Adv Energy Mater* 11:2101126
- Zhang X, Li Z, Luo L, Fan Y, Du Z (2022) A review on thermal management of lithium-ion batteries for electric vehicles. *Energy* 238:121652
- Wu F, Maier J, Yu Y (2020) Guidelines and trends for next-generation rechargeable lithium and lithium-ion batteries. *Chem Soc Rev* 49:1569–1614
- Zhang L, Li X, Yang M, Chen W (2021) High-safety separators for lithium-ion batteries and sodium-ion batteries: advances and perspective. *Energy Storage Mater* 41:522–545
- Abraham K (2020) How comparable are sodium-ion batteries to lithium-ion counterparts? *ACS Energy Lett* 5:3544–3547
- Kim T, Song W, Son D-Y, Ono LK, Qi Y (2019) Lithium-ion batteries: outlook on present, future, and hybridized technologies. *J Mater Chem A* 7:2942–2964
- Duffner F, Kronmeyer N, Tübke J, Leker J, Winter M, Schmüch R (2021) Post-lithium-ion battery cell production and its compatibility with lithium-ion cell production infrastructure. *Nat Energy* 6:123–134
- Fu L, Zhang X, Ding S, Chen F, Lv Y, Zhang H, Zhao S (2022) Recent developments in the electrochemical determination of sulfonamides. *Curr Pharm Anal* 18:4–13. <https://doi.org/10.2174/1573412917999201006195229>
- Grey CP, Hall DS (2020) Prospects for lithium-ion batteries and beyond—a 2030 vision. *Nat Commun* 11:6279
- Zhan R, Wang X, Chen Z, Seh ZW, Wang L, Sun Y (2021) Promises and challenges of the practical implementation of prelithiation in lithium-ion batteries. *Adv Energy Mater* 11:2101565
- Huang C-Y, Kuo T-R, Yougbaré S, Lin L-Y (2022) Design of LiFePO<sub>4</sub> and porous carbon composites with excellent High-Rate charging performance for Lithium-Ion secondary battery. *J Colloid Interface Sci* 607:1457–1465
- Wang Y, Wang X, Jiang A, Liu G, Yu W, Dong X, Wang J (2019) A versatile nitrogen-doped carbon coating strategy to improve the electrochemical performance of LiFePO<sub>4</sub> cathodes for lithium-ion batteries. *J Alloys Compd* 810:151889
- Wang X, Feng Z, Hou X, Liu L, He M, He X, Huang J, Wen Z (2020) Fluorine doped carbon coating of LiFePO<sub>4</sub> as a cathode material for lithium-ion batteries. *Chem Eng J* 379:122371
- Zhang H, Li J, Luo L, Zhao J, He J, Zhao X, Liu H, Qin Y, Wang F, Song J (2021) Hierarchically porous MXene decorated carbon coated LiFePO<sub>4</sub> as cathode material for high-performance lithium-ion batteries. *J Alloys Compd* 876:160210
- Iarchuk AR, Nikitina VA, Karpushkin EA, Sergeyev VG, Antipov EV, Stevenson KJ, Abakumov AM (2019) Influence of carbon coating on intercalation kinetics and transport properties of LiFePO<sub>4</sub>. *ChemElectroChem* 6:5090–5100
- Kim J-K, Jeong SM (2020) Physico-electrochemical properties of carbon coated LiFePO<sub>4</sub> nanoparticles prepared by different preparation method. *Appl Surf Sci* 505:144630
- Lai A, Chu Y, Jiang J, Huang Y, Hu S, Pan Q, Zheng F, Wang J, Li J, Wang H (2022) Self-restriction to form in-situ N, P co-doped carbon-coated LiFePO<sub>4</sub> nanocomposites for high-performance lithium ion batteries. *Electrochim Acta* 414:140161
- Xi Y, Lu Y (2020) Toward uniform in situ carbon coating on nano-LiFePO<sub>4</sub> via a solid-state reaction. *Ind Eng Chem Res* 59:13549–13555
- Wang C, Yuan X, Tan H, Jian S, Ma Z, Zhao J, Wang X, Chen D, Dong Y (2021) Three-dimensional carbon-coated LiFePO<sub>4</sub> cathode with improved Li-ion battery performance. *Coatings* 11:1137
- Liu Z, Zhang R, Xu F, Gao Y, Zhao J (2022) Structure and electrochemical performance of LiFePO<sub>4</sub> cathode materials modified with carbon coating and metal doping. *J Solid State Electrochem* 26:1655–1665
- Ravet N, Chouinard Y, Magnan JF, Besner S, Gauthier M, Armand M (2001) Electroactivity of natural and synthetic triphylite. *Proc 10th Int Meet Lithium Batter* 97–98:503–507. [https://doi.org/10.1016/S0378-7753\(01\)00727-3](https://doi.org/10.1016/S0378-7753(01)00727-3)
- Zhao N, Zhi X, Wang L, Liu Y, Liang G (2015) Effect of microstructure on low temperature electrochemical properties of LiFePO<sub>4</sub>/C cathode material. *J Alloys Compd* 645:301–308. <https://doi.org/10.1016/j.jallcom.2015.05.097>
- Huynh LTN, Nguyen HHA, Tran TTD, Nguyen TTT, Nguyen TMA, La TH, Tran VM, Le MLP (2019) Electrode composite LiFePO<sub>4</sub>@Carbon: structure and electrochemical performances. *J Nanomater* 2019:2464920. <https://doi.org/10.1155/2019/2464920>
- Liu X, Zhao R, Xia Y, Li Q (2022) Improved electrochemical performance of LiFePO<sub>4</sub>/carbon cathode for lithium-ion batteries. *Ionics* 28:4579–4585
- Zhao S, Wen L, Liu J, Chen J, Bei F (2020) Mn-doped LiFePO<sub>4</sub>/C composite with excellent high-rate performance as lithium ion batteries cathode. *Int J Electrochem Sci* 15:8873–8882
- Bai Y-X, Zhang J, Yang Y-B, Yang R, Yan Y-L, Wang J (2020) Enhance electrochemical performance of LiFePO<sub>4</sub> cathode material by Al-doped Li<sub>7</sub>La<sub>3</sub>Zr<sub>2</sub>O<sub>12</sub> and carbon co-coating surface modification. *J Alloys Compd* 843:154915
- Li Y, Wang L, Zhang K, Liang F, Yao Y, Kong L (2022) High performance of LiFePO<sub>4</sub> with nitrogen and phosphorus dual-doped carbon layer for lithium-ion batteries. *J Alloys Compd* 890:161617
- Chen M, Liu F-M, Chen S-S, Zhao Y-J, Sun Y, Li C-S, Yuan Z-Y, Qian X, Wan R (2023) In situ self-catalyzed formation of carbon nanotube wrapped and amorphous nanocarbon shell coated LiFePO<sub>4</sub> microclew for high-power lithium ion batteries. *Carbon* 203:661–670
- Gangaraju V, Shastri M, Shetty K, Marilingaiah NR, Anantharaju K, Shivaramu PD, Rangappa D (2022) In-situ preparation of silk-cocoon derived carbon and LiFePO<sub>4</sub> nanocomposite as cathode material for Li-ion battery. *Ceram Int* 48:35657–35665
- Khan S, Raj RP, George L, Kannagara GK, Milev A, Varadaraju UV, Selvam P (2020) Surfactant-mediated and morphology-controlled nanostructured LiFePO<sub>4</sub>/carbon composite as a promising cathode material for Li-ion batteries. *ChemistryOpen* 9:23–31
- Omidi AH, Babaei A, Ataie A (2020) Low temperature synthesis of nanostructured LiFePO<sub>4</sub>/C cathode material for lithium ion batteries. *Mater Res Bull* 125:110807
- Chen Z, Xu M, Du B, Zhu H, Xie T, Wang W (2014) Morphology control of lithium iron phosphate nanoparticles by

- soluble starch-assisted hydrothermal synthesis. *J Power Sources* 272:837–844
36. Sun S, Yan Q, Wu M, Zhao X (2021) Carbon aerogel based materials for secondary batteries. *Sustain Mater Technol* 30:e00342
  37. Naghib SM, Behzad F, Rahmanian M, Zare Y, Rhee KY (2020) A highly sensitive biosensor based on methacrylated graphene oxide-grafted polyaniline for ascorbic acid determination. *Nano-technol Rev* 9:760–767

**Publisher's Note** Springer Nature remains neutral with regard to jurisdictional claims in published maps and institutional affiliations.

Springer Nature or its licensor (e.g. a society or other partner) holds exclusive rights to this article under a publishing agreement with the author(s) or other rightsholder(s); author self-archiving of the accepted manuscript version of this article is solely governed by the terms of such publishing agreement and applicable law.